International Journal of Bifurcation and Chaos, Vol. 26, No. 13 (2016) 1650213 (11 pages)

DOI: 10.1142/S0218127416502138

A Simplified GCS-DCSK Modulation and Its Performance Optimization

Weikai Xu* and Lin Wang†
The Department of Communication Engineering,
Xiamen University, Xiamen,
Fujian Province 361005, P. R. China
**xweikai@xmu.edu.cn*
†*wanglin@xmu.edu.cn*

Chong-Yung Chi
Department of Electrical Engineering,
National Tsing Hua University, Hsinchu, Taiwan, R.O.C.
cychi@ee.nthu.edu.tw

Received October 9, 2015; Revised September 1, 2016

In this paper, a simplified Generalized Code-Shifted Differential Chaos Shift Keying (GCS-DCSK) whose transmitter never needs any delay circuits, is proposed. However, its performance is deteriorated because the orthogonality between substreams cannot be guaranteed. In order to optimize its performance, the system model of the proposed GCS-DCSK with power allocations on substreams is presented. An approximate bit error rate (BER) expression of the proposed model, which is a function of substreams' power, is derived using Gaussian Approximation. Based on the BER expression, an optimal power allocation strategy between information substreams and reference substream is obtained. Simulation results show that the BER performance of the proposed GCS-DCSK with the optimal power allocation can be significantly improved when the number of substreams M is large.

Keywords: Chaos communications; generalized code-shifted differential chaos shift keying (GCS-DCSK); power allocation; bit error rate (BER).

1. Introduction

Chaotic modulations have been extensively studied where, differing from conventional modulation schemes, a wideband nonperiodic chaotic signal is used as their carrier [Lau & Tse, 2003; Kolumbán, 2000]. Among all the chaos digital modulations, Differential Chaos Shift Keying (DCSK) offers excellent performance for multipath fading or time-varying channels [Kolumbán *et al.*, 1996; Yao & Lawrance, 2006; Yang & Jiang, 2012; Yang *et al.*, 2013, 2014]. As a simple alternative spread-spectrum communication method [Ye *et al.*, 2005], the DCSK modulation has high robustness against multipath fading even in a severe multipath transmission environment. Its hardware complexity advantage has motivated considerable interest to design better wireless personal area networks (WPANs) [Chong & Yong, 2008], Multiple Input Multiple Output (MIMO) and cooperative systems [Fang *et al.*, 2013; Chen *et al.*, 2013; Kaddoum *et al.*, 2011; Kaddoum & Gagnon, 2013; Xu *et al.*, 2011a; Kaddoum *et al.*, 2014], CS-DCSK/BPSK coexistence communication system [Xu *et al.*, 2014a].

Due to wideband power density properties of chaos signals, modulation based on chaos signals is an ideal transmission scheme for Ultra-WideBand

(UWB) communication systems [Chen *et al.*, 2010; Kolumbán, 2002; Min *et al.*, 2010]. However, as a Transmitted-Reference (TR) transmission scheme, Frequency-Modulated Differential Chaos Shift Keying (FM-DCSK) UWB receiver requires an ultra-wideband Radio Frequency (RF) delay circuit which is difficult to implement by low-cost CMOS [Stralen *et al.*, 2002; Casu & Durisi, 2005]. For this reason, some alternative DCSK modulations are proposed [Xu *et al.*, 2011b, 2012], which avoid RF delay circuits at the receiver. The Code-Shifted Differential Chaos Shift Keying (CS-DCSK) [Xu *et al.*, 2011b] and Generalized CS-DCSK (GCS-DCSK) [Xu *et al.*, 2012] modulation schemes apply the orthogonal Walsh codes to reference signal and information bearing signals, respectively. In [Kaddoum & Gagnon, 2012], a high spectral efficiency DCSK system is presented, where chaotic sequences are used instead of the Walsh codes in CS-DCSK. However, it needs synchronization of chaotic sequences, that is a difficult task. In [Kaddoum *et al.*, 2013], the authors proposed a Multi-Carrier DCSK (MC-DCSK) scheme which uses different frequency carriers as reference signal and information bearing signals, respectively. It not only avoids the delay circuits at transmitter and receiver but also enhances the data rate of DCSK. However, the mixers for sine wave modulation and demodulation increase the complexity of MC-DCSK.

In the GCS-DCSK [Xu *et al.*, 2012], a truncated chaos signal was used as the carrier. Although the truncated chaos signal guarantees the orthogonality between the substreams of GCS-DCSK, it results in a complex transmitter which requires multiple delay circuits to delay the truncated chaotic signal. In order to further simplify the transmitter, we propose a simplified GCS-DCSK scheme, referred to as GCS-DCSK-II in this paper, whose transmitter does not need any delay circuits. Then, we derive BER expressions of the proposed system with power allocation on substreams. Since the orthogonality between substreams is not guaranteed in the proposed system, we further improve the performance of the proposed system by optimizing the power allocation on substreams. To improve the performance, using our method in [Xu *et al.*, 2014b], the optimal power allocation strategies for different number of substreams M are obtained. Then, we evaluate the performance of the proposed GCS-DCSK system with optimal power and equal power allocations, respectively. When the number of substreams M is large, the optimal power allocation strategy obtains significant performance over AWGN and Rayleigh multipath fading channels.

The main contributions of this paper are summarized as follows: (1) We propose an improved GCS-DCSK scheme whose transmitter does not require any delay circuits. (2) We analyze its performance and give a closed BER expression in terms of substream power. (3) To minimize BER, we optimize the power allocation on substreams of the proposed GCS-DCSK. Analysis and simulation results show that the optimal power allocation strategy significantly improves the performance of the proposed GCS-DCSK.

The rest of this paper is organized as follows. Section 2 presents the power allocated system model of the proposed GCS-DCSK. In Sec. 3, the desired power allocation strategy is presented. Numerical simulations are presented in Sec. 4. Section 5 concludes the paper.

2. System Model

In [Xu *et al.*, 2012], a Generalized Code-Shifted DCSK (GCS-DCSK) scheme was proposed. In this scheme, a truncated chaos signal with duration T_c is adopted as the carrier. For convenient formulation, we denote it as GCS-DCSK-I. We first define two Walsh functions $w_R(t)$ and $w_{I_m}(t)$ as

$$\begin{aligned} w_R(t) &= \sum_{k=0}^{N-1} w_{R,k+1}\mathrm{rect}(t - kT_c) \\ w_{I_m}(t) &= \sum_{k=0}^{N-1} w_{I_m,k+1}\mathrm{rect}(t - kT_c) \end{aligned} \tag{1}$$

where $w_{R,k}$ and $w_{I_m,k}$ are the orthogonal Walsh code sequences, $\mathrm{rect}(t)$ is a rectangle pulse over the interval $[0, T_c]$ and its energy is normalized to 1. Suppose that $c_1(t)$ is a truncated chaotic signal over the interval $[0, T_c]$ with energy $\mathscr{E}_1 = \mathrm{E}\{c_1^2(t)\}$, where $\mathrm{E}\{\,\}$ is expectation operator. The chaos signal is invariant in a symbol period T_s, but it is changed in different symbol duration. In GCS-DCSK-I [Xu *et al.*, 2012], the same power P_1 is allocated over reference and all information substreams. Assuming single symbol transmitted, the transmitted signal of

GCS-DCSK-I is

$$s_1(t) = \sqrt{P_1} w_R(t) \sum_{k=0}^{N-1} \left[\frac{1}{\sqrt{N\mathscr{E}_1}} c_1(t - kT_c) \right] + \sum_{m=1}^{M} \sqrt{P_1} a_m w_{I_m}(t) \times \sum_{k=0}^{N-1} \left[\frac{1}{\sqrt{N\mathscr{E}_1}} c_1(t - kT_c) \right] \quad (2)$$

where $T_s = NT_c$ and T_c are symbol and frame duration, respectively, M is the number of substreams, N is number of frames in a symbol duration, $a_m \in \{-1, +1\}$ is the mth information symbol ($m = 1, 2, \ldots, M$) carried by the mth information substream, which is mapped from information bit b_m. The transmitter of GCS-DCSK-I needs delay circuits to delay the truncated chaos signal, which results in high complexity.

A simplified GCS-DCSK, denoted by GCS-DCSK-II, is represented in this section. The block diagram of transmitter of the proposed scheme is shown in Fig. 1. Different from the GCS-DCSK-I, GCS-DCSK-II utilizes a nonperiodic chaotic signal with duration T_s as the carrier. Thus the delay circuits used to delay period chaos signal in transmitter of GCS-DCSK-I are avoided. However, its performance will be deteriorated because the orthogonality between substreams cannot be guaranteed. In order to alleviate the effect of substream interference, we study the power allocation on reference substream and information substreams of the proposed GCS-DCSK-II scheme. Our aim is to optimize the power ratio between information substream and reference substream. So we assume

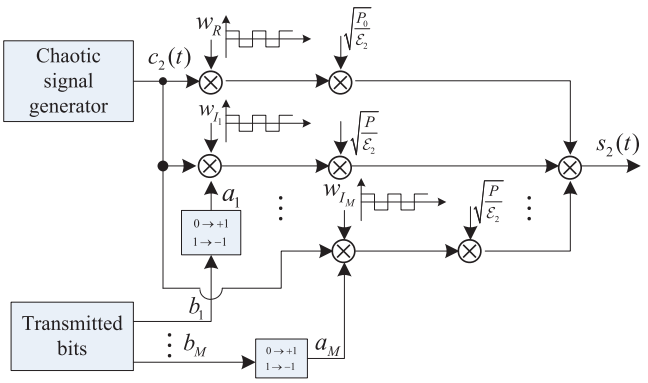

Fig. 1. Block diagram of the GCS-DCSK-II transmitter.

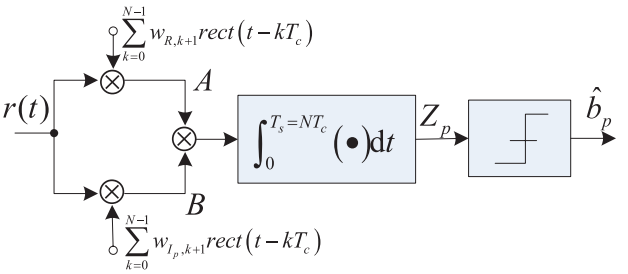

Fig. 2. Block diagram of the pth detector of the GCS-DCSK-II receiver.

that the power of reference substream is P_0, and the power of all information substreams is P. Let $\mathbf{w_R}$ and $\mathbf{w_{I_m}}$ represent reference and the mth substream Walsh code sequences, respectively. So the transmitted signal of GCS-DCSK-II is

$$s_2(t) = \sqrt{\frac{P_0}{\mathscr{E}_2}} [\mathbf{w_R} \otimes \text{rect}(t)] c_2(t) + \sum_{m=1}^{M} a_m \sqrt{\frac{P}{\mathscr{E}_2}} [\mathbf{w_{I_m}} \otimes \text{rect}(t)] c_2(t) \quad (3)$$

where $\otimes$ is Kronecker product, $c_2(t)$ is a chaotic signal over the interval $[0, NT_c]$ with energy $\mathscr{E}_2 = \text{E}\{c_2^2(t)\}$.

We assume that the channel is an ideal Additive White Gaussian Noise (AWGN) channel. Then the received signal $r(t)$ is

$$r(t) = s_2(t) + n(t) \quad (4)$$

where $n(t)$ is zero-mean white Gaussian noise with a two-sided power spectral density $N_0/2$.

The receiver structure of the GCS-DCSK-II is the same as that of GCS-DCSK-I. The block diagram of the pth detector of GCS-DCSK-II receiver is shown in Fig. 2. Thus, the observation statistic of the pth substream at receiver is computed by

$$Z_p = \int_0^{T_s} [w_R(t) r(t)] \times [w_{I_p}(t) r(t)] dt. \quad (5)$$

Then, the pth transmitted bit can be retrieved by the decision rule

$$\hat{b}_p = \begin{cases} 1, & \text{if } Z_p \geq 0 \\ 0, & \text{else } Z_p < 0. \end{cases} \quad (6)$$

Throughout the paper, perfect synchronization is assumed and the synchronization problem will be studied in the future.

3. Performance Optimization

In this section, we first derive the BER expression of GCS-DCSK-II over AWGN channel. Then we optimize the power allocation on reference and information bearing substreams. Our analysis will proceed in a discrete-time equivalent form. We assume that the sampling rate of the receiver is f_s. Thus the number of samples in one frame duration is $\beta = T_c f_s$. The spreading factor ($SF = T_s f_s = N\beta$) is the number of samples in one symbol duration. We employ chaos map $c_{j+1} = 1 - 2c_j^2$ to generate the chaos sequence with sample rate f_s. The mean and the variance of c_j^2 are $\mathrm{E}\{c_j^2\} = 1/2$ and $\mathrm{Var}\{c_j^2\} = 1/8$ [Lau & Tse, 2003], respectively.

Using the notations discussed above, the discrete-time equivalent of (5) is,

$$\begin{aligned} Z_p = &\left(\sqrt{\frac{P_0}{\mathscr{E}_2}}\sum_{k=0}^{N-1} w_{R,k+1}w_{R,k+1}\sum_{j=0}^{\beta-1} c_{k\beta+j} + \sum_{m=1}^{M} a_m\sqrt{\frac{P}{\mathscr{E}_2}}\sum_{k=0}^{N-1} w_{R,k+1}w_{I_m,k+1}\sum_{j=0}^{\beta-1} c_{k\beta+j}\right.\\ &\left.+\sum_{k=0}^{N-1} w_{R,k+1}\sum_{j=0}^{\beta-1} n_{k\beta+j}\right)\left(\sqrt{\frac{P_0}{\mathscr{E}_2}}\sum_{k=0}^{N-1} w_{I_p,k+1}w_{R,k+1}\sum_{j=0}^{\beta-1} c_{k\beta+j}\right.\\ &\left.+\sum_{m=1}^{M} a_m\sqrt{\frac{P}{\mathscr{E}_2}}\sum_{k=0}^{N-1} w_{I_p,k+1}w_{I_m,k+1}\sum_{j=0}^{\beta-1} c_{k\beta+j} + \sum_{k=0}^{N-1} w_{I_p,k+1}\sum_{j=0}^{\beta-1} n_{k\beta+j}\right). \end{aligned} \tag{7}$$

The decision statistic Z_p can be expressed as the sum of three items: "signal cross signal", "signal cross noise" and "noise cross noise",

$$Z_p = Z_{s\times s} + Z_{s\times n} + Z_{n\times n} \tag{8}$$

where

$$\begin{aligned} Z_{s\times s} = &\frac{P_0}{\mathscr{E}_2}\sum_{k=0}^{N-1} w_{R,k+1}w_{I_p,k+1}\sum_{j=0}^{\beta-1} c_{k\beta+j}^2 + \frac{P}{\mathscr{E}_2}a_m^2\sum_{m=1}^{M}\sum_{k=0}^{N-1} w_{R,k+1}w_{I_p,k+1}\sum_{j=0}^{\beta-1} c_{k\beta+j}^2\\ &+\frac{2P}{\mathscr{E}_2}a_m a_l\left(\sum_{m=1}^{M-1}\sum_{l=m+1}^{M}\sum_{k=0}^{N-1} w_{R,k+1}w_{I_p,k+1}w_{I_m,k+1}w_{I_l,k+1}\sum_{j=0}^{\beta-1} c_{k\beta+j}^2\right)\\ &+\frac{2\sqrt{PP_0}}{\mathscr{E}_2}a_m\sum_{m=1,m\neq p}^{M}\sum_{k=0}^{N-1} w_{R,k+1}^2 w_{I_m,k+1}w_{I_p,k+1}\sum_{j=0}^{\beta-1} c_{k\beta+j}^2 + \frac{2\sqrt{PP_0}}{\mathscr{E}_2}a_p\sum_{k=0}^{N-1}\sum_{j=0}^{\beta-1} c_{k\beta+j}^2 \end{aligned} \tag{9}$$

$$\begin{aligned} Z_{s\times n} = &2\sqrt{\frac{P_0}{\mathscr{E}_2}}\sum_{k=0}^{N-1} w_{I_p,k+1}\sum_{j=0}^{\beta-1} c_{k\beta+j}n_{k\beta+j} + 2\sum_{m=1,m\neq p}^{M}\sqrt{\frac{P}{\mathscr{E}_2}}a_m\sum_{k=0}^{N-1} w_{R,k+1}w_{I_p,k+1}w_{I_m,k+1}\sum_{j=0}^{\beta-1} c_{k\beta+j}n_{k\beta+j}\\ &+2\sqrt{\frac{P}{\mathscr{E}_2}}a_p\sum_{k=0}^{N-1} w_{R,k+1}\sum_{j=0}^{\beta-1} c_{k\beta+j}n_{k\beta+j} \end{aligned} \tag{10}$$

$$Z_{n\times n} = \sum_{k=0}^{N-1} w_{R,k+1}w_{I_p,k+1}\sum_{j=0}^{\beta-1} n_{k\beta+j}^2. \tag{11}$$

Bit energy E_b of GCS-DCSK-II is

$$E_b = \frac{(MP + P_0)\sum_{k=0}^{N-1}\sum_{j=0}^{\beta-1} c_{k\beta+j}^2}{M\mathscr{E}_2}. \tag{12}$$

We define

$$B = \sum_{k=0}^{N-1}\sum_{j=0}^{\beta-1} c_{k\beta+j}^2 = \frac{M\mathscr{E}_2 E_b}{MP + P_0}.$$

Due to the orthogonality of Walsh code sequences, except the last term in (9), expected value of the other terms are approximately zero. Thus, given $a_p = +1$, the conditional mean of $[Z_{s\times s}]$ is

$$\begin{aligned}\mathrm{E}\{Z_{s\times s}\} &\approx 2\frac{\sqrt{PP_0}}{\mathscr{E}_2}\sum_{k=0}^{N-1}\sum_{j=0}^{\beta-1}\mathrm{E}\{c_{k\beta+j}^2\}\\ &= 2\frac{\sqrt{PP_0}}{\mathscr{E}_2}N\beta\mathrm{E}\{c_j^2\}. \end{aligned} \tag{13}$$

Because signal and noise are statistically independent, we have

$$\mathrm{E}\{Z_{s\times n}\} = 0. \tag{14}$$

Because orthogonality between Walsh code $\mathbf{w_R}$ and $\mathbf{w_{I_p}}$, we have

$$\mathrm{E}\{Z_{n\times n}\} = 0. \tag{15}$$

Therefore, the conditional mean of Z_p is given by

$$\mathrm{E}\{Z_p \,|\, a_p = +1\} = 2\frac{\sqrt{PP_0}}{\mathscr{E}_2}N\beta\mathrm{E}[c_j^2]. \tag{16}$$

Given $a_p = +1$, the conditional variance of $Z_{s\times s}$ can be obtained as

$$\begin{aligned}&\mathrm{Var}\{Z_{s\times s}\}\\ &\quad= \frac{1}{\mathscr{E}_2^2}\left[4PP_0 + 4P^2\frac{M^2 - M}{2}\right.\\ &\qquad\left. + 4PP_0(M-1) + P_0^2 + P^2M\right]\mathrm{Var}\{B\}\\ &\quad= \frac{1}{\mathscr{E}_2^2}(2M^2P^2 - MP^2 + 4MPP_0 + P_0^2)N\beta\\ &\qquad\times \mathrm{Var}\{c_j^2\}. \end{aligned} \tag{17}$$

The conditional variance of $Z_{s\times n}$ is calculated by,

$$\begin{aligned}\mathrm{Var}\{Z_{s\times n}\} &= 4\frac{P_0}{\mathscr{E}_2}\mathrm{E}\{B\}\frac{N_0}{2} + 4M\frac{P}{\mathscr{E}_2}\mathrm{E}\{B\}\frac{N_0}{2}\\ &= 4P_0\frac{ME_b}{P_0 + PM}\frac{N_0}{2}\\ &\quad + 4MP\frac{ME_b}{P_0 + PM}\frac{N_0}{2}. \end{aligned} \tag{18}$$

The conditional variance of $Z_{n\times n}$ is [Goeckel & Zhang, 2007]

$$\mathrm{Var}\{Z_{n\times n}\} = N\beta\frac{N_0^2}{2}. \tag{19}$$

Therefore, given $a_p = +1$, the conditional variance of Z_p is calculated by

$$\begin{aligned}\mathrm{Var}\{Z_p\} &= \mathrm{Var}\{Z_{s\times s}\} + \mathrm{Var}\{Z_{s\times n}\} + \mathrm{Var}\{Z_{n\times n}\}\\ &\quad + 2\,\mathrm{cov}(Z_{s\times s}, Z_{s\times n}) + 2\,\mathrm{cov}(Z_{s\times s}, Z_{n\times n})\\ &\quad + 2\,\mathrm{cov}(Z_{s\times n}, Z_{n\times n}). \end{aligned} \tag{20}$$

The covariance between $Z_{s\times s}$ and $Z_{s\times n}$ can be calculated by

$$\begin{aligned}&\mathrm{cov}(Z_{s\times s}, Z_{s\times n})\\ &\quad= \mathrm{E}\{Z_{s\times s}Z_{s\times n}\} - \mathrm{E}\{Z_{s\times s}\}\mathrm{E}\{Z_{s\times n}\}\\ &\quad= \mathrm{E}\{Z_{s\times s}Z_{s\times n}\}. \end{aligned} \tag{21}$$

Substituting (14) into (21), (21) can be rewritten by

$$\begin{aligned}\mathrm{cov}(Z_{s\times s}, Z_{s\times n}) &= \mathrm{E}\{Z_{s\times s}Z_{s\times n}\}\\ &\approx \mathrm{E}\left\{\frac{4P_0\sqrt{P}}{\mathscr{E}_2^{3/2}}\sum_{k=0}^{N-1} w_{I_p,k+1}\rho(k) + \frac{4P\sqrt{P_0}}{\mathscr{E}_2^{3/2}}\right.\\ &\quad\times\left.\left(\sum_{m=1,m\neq p}^{M}\sqrt{\frac{P}{\mathscr{E}_2}}a_m\sum_{k=0}^{N-1} w_{R,k+1}w_{I_p,k+1}w_{I_m,k+1}\rho(k)\right) + \frac{4P\sqrt{P_0}}{\mathscr{E}_2^{3/2}}\sum_{k=0}^{N-1} w_{R,k+1}\rho(k)\right\}\\ &= \frac{4P_0\sqrt{P}}{\mathscr{E}_2^{3/2}}\sum_{k=0}^{N-1} w_{I_p,k+1}\mathrm{E}\{\rho(k)\} \end{aligned}$$

$$+\frac{4P\sqrt{P_0}}{\mathscr{E}_2^{3/2}}\left(\sum_{m=1,m\neq p}^{M}\sqrt{\frac{P}{\mathscr{E}_2}}a_m\sum_{k=0}^{N-1}w_{R,k+1}w_{I_p,k+1}w_{I_m,k+1}\mathrm{E}\{\rho(k)\}\right)$$

$$+\frac{4P\sqrt{P_0}}{\mathscr{E}_2^{3/2}}\sum_{k=0}^{N-1}w_{R,k+1}\mathrm{E}\{\rho(k)\}$$

$$=0 \tag{22}$$

where $\rho(k)=\sum_{j=0}^{\beta-1}c_{k\beta+j}^3 n_{k\beta+j}$, the last equality is because chaos signal c_j and noise n_j are statistically independent in (22), and the mean of noise is zero. Similarly, the covariance between $Z_{s\times s}$ and $Z_{n\times n}$ is calculated by

$$\begin{aligned}\mathrm{cov}(Z_{s\times s},Z_{n\times n})&=\mathrm{E}\{Z_{s\times s}Z_{n\times n}\}-\mathrm{E}\{Z_{s\times s}\}\mathrm{E}\{Z_{n\times n}\}\\&=\mathrm{E}\{Z_{s\times s}Z_{n\times n}\}\\&\approx\mathrm{E}\left\{\frac{2\sqrt{PP_0}}{\mathscr{E}_2}a_p\sum_{k=0}^{N-1}w_{R,k+1}w_{I_p,k+1}\sum_{j=0}^{\beta-1}c_{k\beta+j}^2n_{k\beta+j}^2\right\}\\&=\frac{2\sqrt{PP_0}}{\mathscr{E}_2}a_p\sum_{k=0}^{N-1}w_{R,k+1}w_{I_p,k+1}\sum_{j=0}^{\beta-1}\mathrm{E}\{c_{k\beta+j}^2\}\mathrm{E}\{n_{k\beta+j}^2\}.\end{aligned} \tag{23}$$

Using the orthogonality of Walsh code, (23) is approximately zero.

The covariance between $Z_{s\times n}$ and $Z_{n\times n}$ is calculated by

$$\begin{aligned}\mathrm{cov}(Z_{s\times n},Z_{n\times n})&=\mathrm{E}\{Z_{s\times n}Z_{n\times n}\}-\mathrm{E}\{Z_{s\times n}\}\mathrm{E}\{Z_{n\times n}\}\\&=\mathrm{E}\{Z_{s\times n}Z_{n\times n}\}\\&=\mathrm{E}\left\{2\sqrt{\frac{P_0}{\mathscr{E}_2}}\sum_{k=0}^{N-1}w_{I_p,k+1}\sum_{j=0}^{\beta-1}c_{k\beta+j}n_{k\beta+j}^3+2\sqrt{\frac{P}{\mathscr{E}_2}}a_p\sum_{k=0}^{N-1}w_{R,k+1}\sum_{j=0}^{\beta-1}c_{k\beta+j}n_{k\beta+j}^2\right.\\&\quad\left.+2\sum_{m=1,m\neq p}^{M}\sqrt{\frac{P}{\mathscr{E}_2}}a_m\sum_{k=0}^{N-1}w_{R,k+1}w_{I_p,k+1}w_{I_m,k+1}\sum_{j=0}^{\beta-1}\mathrm{E}\{c_{k\beta+j}\}\mathrm{E}\{n_{k\beta+j}^3\}\right\}\\&=2\sqrt{\frac{P_0}{\mathscr{E}_2}}\sum_{k=0}^{N-1}w_{I_p,k+1}\sum_{j=0}^{\beta-1}\mathrm{E}\{c_{k\beta+j}\}\mathrm{E}\{n_{k\beta+j}^3\}+2\sqrt{\frac{P}{\mathscr{E}_2}}a_p\sum_{k=0}^{N-1}w_{R,k+1}\sum_{j=0}^{\beta-1}\mathrm{E}\{c_{k\beta+j}\}\mathrm{E}\{n_{k\beta+j}^3\}\\&\quad+2\sum_{m=1,m\neq p}^{M}\sqrt{\frac{P}{\mathscr{E}_2}}a_m\sum_{k=0}^{N-1}w_{R,k+1}w_{I_p,k+1}w_{I_m,k+1}\sum_{j=0}^{\beta-1}\mathrm{E}\{c_{k\beta+j}\}\mathrm{E}\{n_{k\beta+j}^3\}=0\end{aligned} \tag{24}$$

where the last equality is because chaos signal c_j and noise n_j are statistically independent in (24), and the mean of chaos signal c_j is zero.

Substituting (17)–(19), (22)–(24) into (20), the variance of Z_p conditioned on $a_p=1$ is given by

$$\begin{aligned}\mathrm{Var}\{Z_p\,|\,a_p=+1\}&=\frac{1}{\mathscr{E}_2^2}(2M^2P^2-MP^2+4MPP_0+P_0^2)N\beta\,\mathrm{Var}\{c_j^2\}\\&\quad+4P_0\frac{ME_b}{P_0+PM}\frac{N_0}{2}+4MP\frac{ME_b}{P_0+PM}\frac{N_0}{2}+N\beta\frac{N_0^2}{2}.\end{aligned} \tag{25}$$

According to Gaussian Approximation (GA) for the random variable Z_p under $a_p = 1$ or $a_p = -1$, assuming that transmitted bits are equiprobable, the BER is

$$\begin{aligned}\text{BER} &= \frac{1}{2}\Pr(Z_p < 0 \,|\, a_p = +1) + \frac{1}{2}\Pr(Z_p \geq 0 \,|\, a_p = -1) \\ &= \frac{1}{2}\operatorname{erfc}\left(\frac{\mathrm{E}\{Z_p \,|\, a_p = +1\}}{\sqrt{2\,\mathrm{Var}\{Z_p \,|\, a_p = +1\}}}\right) \\ &= \frac{1}{2}\operatorname{erfc}\left(\left[\frac{2\dfrac{N\beta\,\mathrm{Var}[c_j^2]}{\mathscr{E}_2^2}(2M^2P^2 - MP^2 + 4MPP_0 + P_0^2)}{4\dfrac{PP_0}{\mathscr{E}_2^2}N^2\beta^2\mathrm{E}^2[c_j^2]}\right.\right. \\ &\quad \left.\left. + \frac{4E_bN_0M(P_0 + MP)^2 + (P_0 + MP)^2N\beta N_0^2}{4PP_0M^2E_b^2}\right]^{-\frac{1}{2}}\right)\end{aligned} \tag{26}$$

where $\operatorname{erfc}(\cdot)$ denotes the complementary error function. Substituting $\mathrm{E}\{c_j^2\} = 1/2$ and $\mathrm{Var}\{c_j^2\} = 1/8$ into (26), the BER expression can be obtained as

$$\begin{aligned}\text{BER} = \frac{1}{2}\operatorname{erfc}\left(\left[\frac{(2M^2 - M)P^2 + 4MPP_0 + P_0^2}{4N\beta PP_0}\right.\right. \\ + 2\frac{N_0}{E_b} + \left(\frac{P_0}{MP} + \frac{MP}{P_0}\right)\frac{N_0}{E_b} \\ \left.\left. + \frac{1}{4}\left(\frac{P_0}{M^2P} + \frac{2}{M} + \frac{P}{P_0}\right)N\beta\frac{N_0^2}{E_b^2}\right]^{-\frac{1}{2}}\right).\end{aligned} \tag{27}$$

Let $\lambda = P/P_0$, and we define $\Phi(N_0/E_b, \lambda)$ as

$$\begin{aligned}&\Phi\left(\frac{N_0}{E_b}, \lambda\right) \\ &= \left[\frac{(2M^2 - M)}{4N\beta} + M\frac{N_0}{E_b} + \frac{N\beta}{4}\left(\frac{N_0}{E_b}\right)^2\right]\lambda \\ &\quad + \left[\frac{1}{4N\beta} + \frac{1}{M}\frac{N_0}{E_b} + \frac{N\beta}{4M^2}\left(\frac{N_0}{E_b}\right)^2\right]\lambda^{-1} \\ &\quad + \frac{M}{N\beta} + \frac{2N_0}{E_b} + \frac{N\beta}{2M}\left(\frac{N_0}{E_b}\right)^2.\end{aligned} \tag{28}$$

Note that minimizing $\text{BER} = \operatorname{erfc}(\Phi(N_0/E_b, \lambda)^{-1/2})$ is equivalent to minimizing $\Phi(N_0/E_b, \lambda)^{-1/2}$. Since $\Phi(N_0/E_b, \lambda)$ is a convex function, the optimal λ^* of minimizing $\Phi(N_0/E_b, \lambda)$ that satisfies $\frac{d\Phi(N_0/E_b,\lambda)}{d\lambda} = 0$ can be shown to be

$$\lambda^* = \sqrt{\frac{\left(\dfrac{E_b}{N_0}\right)^2 + \dfrac{4N\beta}{M}\dfrac{E_b}{N_0} + \left(\dfrac{N\beta}{M}\right)^2}{(2M^2 - M)\left(\dfrac{E_b}{N_0}\right)^2 + 4MN\beta\dfrac{E_b}{N_0} + (N\beta)^2}}. \tag{29}$$

For an L-path Rayleigh multipath fading channel with gain α_l for the lth path, the instantaneous signal-to-noise ratio (SNR) per bit at the receiver can be written as,

$$r_b \approx \frac{E_b}{N_0}\sum_{l=1}^{L}\alpha_l^2. \tag{30}$$

According to [Xia *et al.*, 2004], the averaged unconditional BER of the systems over multipath fading channel is given by

$$\overline{\text{BER}} = \int_0^\infty \frac{1}{2}\operatorname{erfc}(\Phi'(r_b, \lambda))f(r_b)dr_b \tag{31}$$

where $f(r_b)$ is probability density function of the received instantaneous SNR r_b, which is independent of λ. Thus, for given r_b, M and spread factor $N\beta$, the optimal ratio λ^* is obtained by minimizing the function $\Phi'(r_b, \lambda)$, which is the same with the AWGN case except for E_b/N_0 replaced by r_b.

4. Results and Discussions

To evaluate the effect of the power of substreams on the system performance, the analyzed BER and simulation results of the GCS-DCSK-II system over AWGN and Rayleigh multipath fading channels are illustrated.

Figures 3 and 4 depict the BER versus power ratio λ for $\beta = 60$ and $\beta = 20$, respectively. The real lines show analyzed results from (26) and dots are simulation results. It is shown that the analyzed results are in good agreement with the simulations when β is 60. Figure 4 also shows that the simulation results are not in good agreement with the analysis counterpart when M is large and β is small. This is because the Gaussian Approximation method is accurate only for sufficiently large spreading factor. It also shows that the minimum BERs of different M are almost same for the optimal power allocation scheme, but there are large gaps if the reference and information substreams have equal power (i.e. $\lambda = 1$). Thus, the optimal power allocation strategy obtains larger gains for larger M. For example, given $\beta = 60$ and $E_b/N_0 = 15\,\text{dB}$, almost the same minimum BER 2.2×10^{-3} is obtained, and the corresponding optimal power ratios $\lambda^* \approx 0.0618$, 0.1237, 0.2478 for $M = 16, 8, 4$, respectively.

Figure 5 plots the effect of substreams power allocation strategy on BER under an AWGN channel. In this figure, the optimal power ratio λ^* is obtained by (29) with $\beta = 60$ and given E_b/N_0 from 0 dB to 22 dB for $M = 2, 4, 8, 16, 64, 128$ and 256,

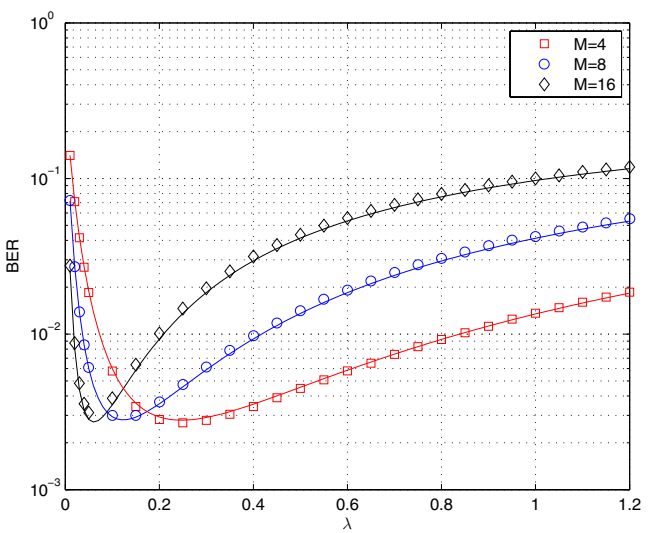

Fig. 3. BER versus power ratio λ over AWGN channel for analysis and simulation, $E_b/N_0 = 15\,\text{dB}$, $\beta = 60$.

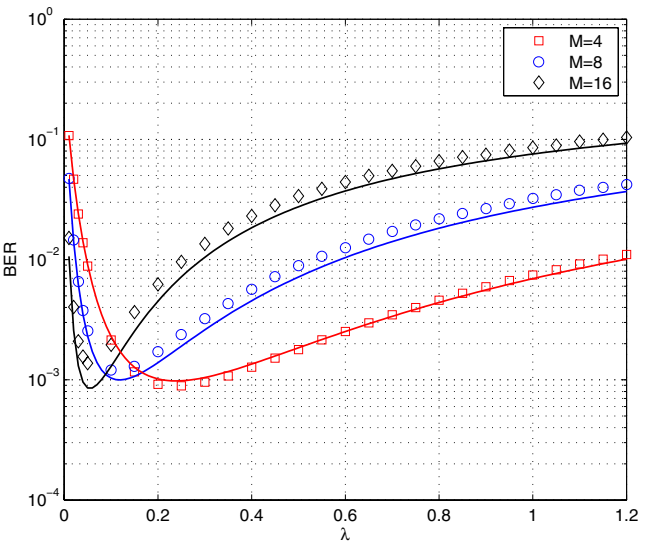

Fig. 4. BER versus power ratio λ over AWGN channel for analysis and simulation, $E_b/N_0 = 15\,\text{dB}$, $\beta = 20$.

respectively. The corresponding results of GCS-DCSK-I and GCS-DCSK-II whose reference substream power equals information substreams power are also presented. They are denoted as black dash lines and blue dash-dot lines in Fig. 5, respectively. When the number of substreams is small, the performance enhancement is limited. For example, the BER curves almost overlay for $M = 2$. However, the performance gains are obvious when the number of substreams M is large. For example, the BER level

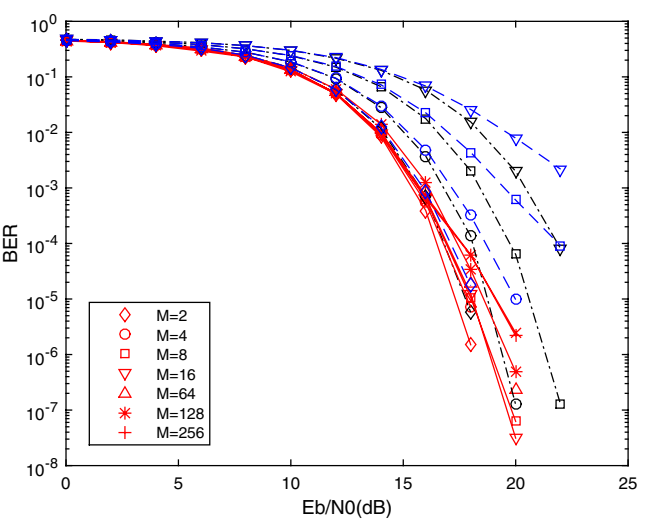

Fig. 5. BER performance comparisons of optimal power allocation and equal power allocation over AWGN channel, $\beta = 60$. Red lines, black dash lines and blue dash-dot lines represent optimal power allocated GCS-DCSK-II, GCS-DCSK-I and GCS-DCSK-II with equal power on substreams, respectively.

can be significantly dropped to 10^{-7} with $\lambda = \lambda^*$ for $E_b/N_0 = 20\,\text{dB}$, but it is about 10^{-2} when the power ($\lambda = 1$) is equal in reference substream and information substreams for $M = 16$. In addition, the performances of power allocated GCS-DCSK-II are better than that of the GCS-DCSK-I whose substreams are orthogonal to each other.

The performance comparisons of the GCS-DCSK-II and GCS-DCSK-I over Rayleigh multipath fading channels are illustrated in Figs. 6 and 7. We consider a dense resolvable multipath channel, where each multipath gain is Rayleigh distributed with path average power $\mathrm{E}\{\alpha_l^2\}$, where $\mathrm{E}\{\alpha_l^2\} = \mathrm{E}\{\alpha_1^2\}\exp[-e(l-1)]$, for $l = 1, 2, \ldots, L$, are normalized such that $\sum_{l=1}^{L} \mathrm{E}\{\alpha_l^2\} = 1$. In Fig. 6, the channel impulse response is a 3-path channel with equal average power gain $\mathrm{E}\{\alpha_1^2\} = \mathrm{E}\{\alpha_2^2\} = \mathrm{E}\{\alpha_3^2\} = 1/3$, i.e. $(L, \varepsilon) = (3, 0)$, and path delay $\tau_1 = 0$, $\tau_2 = t_s$, and $\tau_3 = 2t_s$, where t_s is duration of chaos sample interval. For power allocated GCS-DCSK-II, the optimal power ratios are similar to that under AWGN channel. When the number of substreams is small, for example $M = 2$, there is almost no performance enhancement. However, the performance gains are enlarged with M increased. For example, when the number of substreams is $M = 16$, the BER of equal power GCS-DCSK-II and GCS-DCSK-I can only reach about 10^{-1}, however, the BER of optimal power allocated

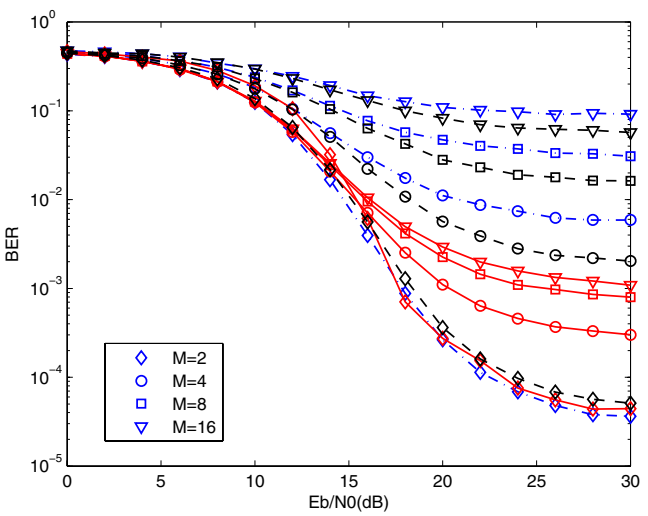

Fig. 6. BER performance comparisons of optimal power allocation and equal power allocation over Rayleigh fading channel, $\beta = 60$. Red lines, black dash lines and blue dash-dot lines represent optimal power allocated GCS-DCSK-II, GCS-DCSK-I and GCS-DCSK-II with equal power on substreams, respectively. Channel parameter is $L = 3$, $\varepsilon = 0$.

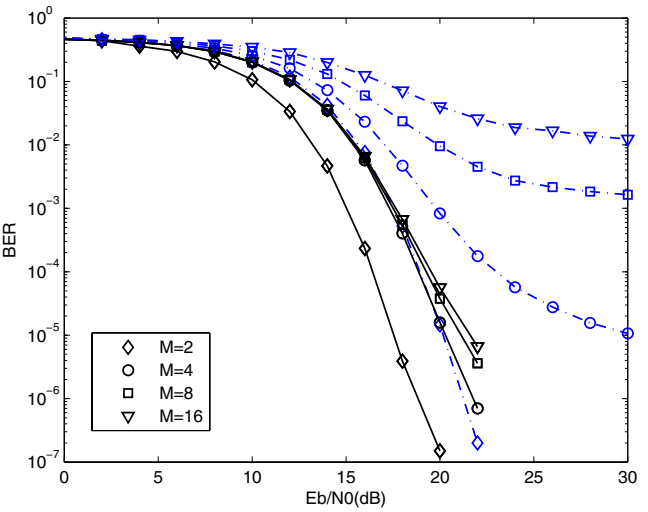

Fig. 7. BER performance comparisons of optimal power allocation and equal power allocation over Rayleigh fading channel, $\beta = 60$. Black dash lines and blue dash-dot lines represent optimal power and equal power allocation on substreams of GCS-DCSK-II, respectively. Channel parameter is $L = 3$, $\varepsilon = 0.4$.

GCS-DCSK-II can drop to 10^{-3} for $E_b/N_0 = 25\,\text{dB}$. In Fig. 7, the channel average power is exponential distribution, i.e. $(L, \varepsilon) = (3, 0.4)$, and path delay $\tau_1 = 0$, $\tau_2 = t_s$, and $\tau_3 = 2t_s$. Similar to equal path average power gain, Fig. 7 apparently shows the superior BER performance of the optimal power allocation strategy over the equal power strategy. It can also be observed that there is no error floor for optimal power allocation.

To understand the effect of synchronization error of Walsh code on BER performance, we plot

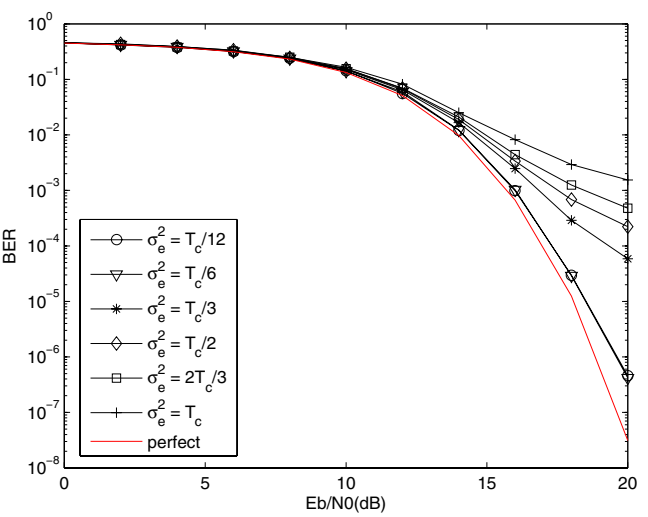

Fig. 8. BER performance of nonperfect synchronization receiving over AWGN channel, $\beta = 60$, $M = 16$.

the BER of GCS-DCSK-II with timing error of Walsh code synchronization in Fig. 8. We assume that the timing error is a normal distributed random variable with zero mean and variance σ_e^2. Figure 8 shows that the BER is increased with the increasing of timing error variance. When the variance is less than $T_c/6$, the BER gap between perfect synchronization and nonperfect synchronization with timing error is negligible. Although the BER is significantly deteriorated when timing error variance is large, there is no obvious error floor when timing error variance is as large as frame interval of T_c. It indicates that the GCS-DCSK-II has good robustness against the timing error. This property will decrease the requirement of timing precision of Walsh code at receiver, thereby relieving the complexity and difficulty of the receiver design.

5. Conclusion

We have presented a simplified GCS-DCSK modulation which uses a continuous chaotic signal as its carrier, and thus the delay circuits in the transmitter are eliminated. In order to enhance BER performance of the proposed scheme, we analyzed the power allocation on substreams of proposed system and derived the associated closed-form BER expression. Optimal power ratios exist between information and reference substream for the proposed GCS-DCSK for different number of substreams M. Simulation results have demonstrated that the BER performance improvement using the optimal power strategy is larger for larger M. The proposed GCS-DCSK with simplified transmitter is more suitable for low-cost applications, such as Wireless Body Area Networks (WBANs).

References

Casu, M. & Durisi, G. [2005] "Implementation aspects of a transmitted-reference UWB receiver," *Wireless Commun. Mobile Comput.* **5**, 537–549.

Chen, S., Wang, L. & Chen, G. [2010] "Data-aided timing synchronization for FM-DCSK UWB communication systems," *IEEE Trans. Ind. Electron.* **57**, 1538–1545.

Chen, P., Wang, L. & Lau, F. C. M. [2013] "One analog STBC-DCSK transmission scheme not requiring channel state information," *IEEE Trans. Circuits Syst.-I* **60**, 1027–1037.

Chong, C. C. & Yong, S. K. [2008] "UWB direct chaotic communication technology for low-rate WPAN applications," *IEEE Trans. Vehic. Technol.* **57**, 1527–1536.

Fang, Y., Xu, J., Wang, L. & Chen, G. [2013] "Performance of MIMO relay DCSK-CD systems over Nakagami fading channels," *IEEE Trans. Circuits Syst.-I* **60**, 757–767.

Goeckel, D. L. & Zhang, Q. [2007] "Slightly frequency-shifted reference Ultra-Wideband (UWB) radio," *IEEE Trans. Commun.* **55**, 508–519.

Kaddoum, G., Vu, M. & Gagnon, F. [2011] "Performance analysis of differential chaotic shift keying communications in MIMO systems," *2011 IEEE Int. Symp. Circuits and Systems*, pp. 1580–1583.

Kaddoum, G. & Gagnon, F. [2012] "Design of a high-data-rate differential chaos-shift keying system," *IEEE Trans. Circuits Syst.-II* **59**, 448–452.

Kaddoum, G. & Gagnon, F. [2013] "Performance analysis of STBC-CSK communication system over slow fading channel," *Sign. Process.* **93**, 2055–2060.

Kaddoum, G., Richardson, F. & Gagnon, F. [2013] "Design and analysis of a multi-carrier differential chaos shift keying communication system," *IEEE Trans. Commun.* **61**, 3281–3291.

Kaddoum, G., Parzysz, F. & Shokraneh, F. [2014] "Low complexity amplify-and-forward relaying protocol for non-coherent chaos-based communication system," *IET Commun.* **8**, 2281–2289.

Kolumbán, G., Vizvari, B., Schwarz, W. & Abel, A. [1996] "Differential chaos shift keying: A robust coding for chaotic communication," *Proc. NDES* **1**, 87–92.

Kolumbán, G. [2000] "Theoretical noise performance of correlator-based chaotic communications schemes," *IEEE Trans. Circuits Syst.-I* **47**, 1692–1701.

Kolumbán, G. [2002] "UWB technology: Chaotic communications versus noncoherent impulse radio," *Proc. ECCTD* **1**, 79–82.

Lau, F. C. M. & Tse, C. K. [2003] *Chaos-Based Digital Communication Systems*: *Operating Principles*, *Analysis Methods*, *and Performance Evaluation* (Springer-Verlag, Berlin).

Min, X., Xu, W., Wang, L. & Chen, G. [2010] "Promising performance of an FM-DCSK UWB system under indoor environments," *IET Commun.* **4**, 125–134.

Stralen, N. V., Dentinger, A., Welles, K., Gans, R., Hoctor, R. & Tomlinson, H. [2002] "Delay hopped transmitted reference experimental results," *IEEE Conf. Ultra Wideband Systems and Technologies*, 2002. Digest of Papers, pp. 93–98.

Xia, Y., Tse, C. K. & Lau, F. C. M. [2004] "Performance of differential chaos-shift-keying digital communication systems over a multipath fading channel with delay spread," *IEEE Trans. Circuits Syst.-II* **51**, 680–684.

Xu, W., Wang, L. & Chen, G. [2011a] "Performance of DCSK cooperative communication systems over multipath fading channels," *IEEE Trans. Circuits Syst.-I* **58**, 196–204.

Xu, W., Wang, L. & Kolumbán, G. [2011b] "A novel differential chaos shift keying modulation scheme," *Int. J. Bifurcation and Chaos* **21**, 799–814.

Xu, W., Wang, L. & Kolumbán, G. [2012] "A new data rate adaption communications scheme for code-shifted differential chaos shift keying modulation," *Int. J. Bifurcation and Chaos* **22**, 1–8.

Xu, W., Wang, L. & Chen, G. [2014a] "Performance analysis of the CS-DCSK/BPSK communication system," *IEEE Trans. Circuits Syst.* **61**, 2624–2633.

Xu, W., Wang, L. & Huang, T. [2014b] "Optimal power allocation in MC-DCSK communication system," *2014 14th Int. Symp. Communications and Information Technologies*, pp. 313–317.

Yang, H. & Jiang, G. [2012] "High-efficiency differential-chaos-scheme for chaos-based noncoherent communication," *IEEE Trans. Circuits Syst.-II* **59**, 312–316.

Yang, H., Jiang, G. & Duan, J. [2013] "Reference-modulated DCSK: A novel chaotic communication scheme," *IEEE Trans. Circuits Syst.-II* **60**, 232–236.

Yang, H., Jiang, G. & Duan, J. [2014] "Phase-separated DCSK: A simple delay-component-free solution for chaotic communications," *IEEE Trans. Circuits Syst.-II* **61**, 967–971.

Yao, J. & Lawrance, A. J. [2006] "Performance analysis and optimization of multi-user differential chaos-shift keying communication systems," *IEEE Trans. Circuits Syst.-I* **53**, 2075–2091.

Ye, L., Chen, G. & Wang, L. [2005] "Essence and advantages of FM-DCSK technique versus traditional spreading spectrum communication method," *J. Circuits Syst. Sign. Process.* **24**, 657–673.